

**Please use the following citation:**

S.E.L. Detiger, R.J.W. Hoogendoorn, A.J. van der Veen, B.J. van Royen, M.N. Helder, G.H. Koenderink and T.H. Smit

*Biomechanical and rheological characterisation of mild intervertebral disc degeneration in a large animal model*

J. Orthop. Res. **31**, 703–709 (2013).

BIOMECHANICAL AND RHEOLOGICAL CHARACTERISATION OF MILD  
INTERVERTEBRAL DISC DEGENERATION IN A LARGE ANIMAL MODEL

Suzanne E.L. Detiger, MD<sup>1,3</sup>, Roel J.W. Hoogendoorn, MD, PhD<sup>1</sup>, Albert J. van der Veen,  
PhD<sup>2,3</sup>, Barend J. van Royen, MD, PhD<sup>1,3</sup>, Marco N. Helder, PhD<sup>1,3</sup>, Gijsje H. Koenderink,  
PhD<sup>4</sup>, Theo H. Smit, PhD<sup>\*,1,3</sup>

<sup>1</sup>Department of Orthopaedic Surgery, VU University Medical Center, Amsterdam

<sup>2</sup>Department of Physics and Medical Technology, VU University Medical Center, Amsterdam

<sup>3</sup>Skeletal Tissue Engineering Group Amsterdam (STEGA) and Research Institute MOVE,  
The Netherlands

<sup>4</sup>FOM Institute AMOLF, Amsterdam

The Netherlands

**\* Corresponding author**

T.H. Smit, PhD

Department of Orthopaedic Surgery

VU University Medical Center

De Boelelaan 1117

1081 HV, Amsterdam, the Netherlands

Tel +31204442988 / Fax +31204442357

e-mail: [th.smit@vumc.nl](mailto:th.smit@vumc.nl)

Running title: FUNCTIONAL CHARACTERISATION OF DISC DEGENERATION

## **Abstract**

Biomechanical properties of healthy and degenerated nucleus pulposus (NP) are thought to be important for future regenerative strategies for intervertebral disc (IVD) repair. However, which specific properties are pivotal as design criteria when developing NP replacement materials is ill understood. Therefore, the purpose of this study was to determine and compare segmental biomechanics and NP viscoelastic properties in normal and mildly degenerated discs. In eight goats, three lumbar IVDs were chemically degenerated using Chondroitinase ABC (CABC), confirmed with radiography and MRI after sacrifice 12 weeks post-operative. Neutral zone (NZ) stiffness and range of motion (ROM) were determined sagittally, laterally and rotationally for each spinal motion segment (SMS) using a mechanical testing device. NPs were isolated for oscillatory shear experiments; elastic and viscous shear moduli followed from the ratio between shear stress and strain. Water content was quantified by weighing before and after freeze-drying. Disc height on radiographs and signal intensity on MRI decreased (6% and 22%,  $p < 0.01$ ) after CABC treatment, confirming that chemical degeneration provides a good model of disc degeneration. Furthermore, CABC-injected IVDs had significantly lower NZ stiffness and larger ROM in lateral bending and axial rotation than controls. Rheometry consistently revealed significantly lower (10-12%) viscoelastic moduli after mild degeneration within goats, though the inter-animal differences were relatively large (complex modulus ~12-41 kPa). Relative water content in the NP was unaffected by CABC, remaining at ~75%. These observations suggest that viscoelastic properties have a marginal influence on mechanical behaviour of the whole spinal motion segment. Therefore, when developing replacement materials the focus should be on other design criteria, such as biochemical cues and swelling pressure.

**Keywords:** nucleus pulposus; biomechanics; viscoelasticity; animal model; disc degeneration

## **Introduction**

Low back pain is attributable to multiple biological, psychological, and socioeconomic factors, among which intervertebral disc (IVD) degeneration plays an important etiological role.<sup>1-3</sup> As degeneration appears to start with changes in the nucleus pulposus (NP),<sup>4</sup> several research groups have been working on strategies for NP regeneration.<sup>5-9</sup> Different cell types have been identified as potential therapeutic candidates for disc regeneration, including chondrocytes, nucleus pulposus cells and mesenchymal stem cells (MSCs).<sup>10,11</sup> The behaviour of these regenerative cells is known to be governed by biochemical (pH, oxygen and glucose levels)<sup>12,13</sup> as well as mechanical stimuli<sup>14</sup>. More specifically, these cells have all been shown to react differently to varying degrees of stiffness of their substrates, in terms of differentiation<sup>15-17</sup>, proliferation and migration<sup>18</sup> as well as matrix production<sup>19</sup>. Therefore, regeneration strategies often aim to mimic the specific environment of the native, healthy NP tissue by introducing replacement materials combined with regenerative cells. However, the conditions in the degenerated IVD are also relevant, as they represent the environment that will influence the capacity of newly introduced cells.

One of the defining factors of this environment is the viscoelasticity of the surrounding matrix, measured as the mechanical response to dynamic shear load. These properties have only recently been marginally addressed in cadaveric human<sup>20</sup> and animal<sup>21</sup> studies on NP material, but not yet in a reproducible disc degeneration model. Furthermore, bending and torsion loading of a whole spinal motion segment importantly influences the intervertebral disc. Therefore, the objective of this study was to determine both, biomechanical characteristics of the whole spinal motion segment, and viscoelastic properties of the NP in healthy and mildly degenerated discs. For this purpose we used a goat model of chemically induced mild intervertebral disc degeneration which was established in earlier studies by our group.<sup>22,23</sup>

## **Materials and Methods**

### ***Animals and Surgical Procedure***

Eight skeletally mature female Dutch milk goats (age 3-4 years, weight  $92 \pm 10$  kg) were obtained from a local farmer. The research protocol was approved by both the Scientific Board and the Animal Ethics Committee of the VU University Medical Center in Amsterdam. To establish mild degeneration, 3 out of 6 lumbar IVDs in each goat were injected with the enzyme Chondroitinase ABC (CABC) which cleaves proteoglycans, thereby providing the onset of the degenerative cascade. Goats were operated using the same procedure as described before.<sup>22,23</sup> Briefly, lumbar IVDs were approached through a dorsal left paravertebral incision and exposed after mobilisation of the psoas muscle. CABC (Sigma Aldrich Inc., St. Louis, MO) was dissolved in phosphate buffered saline (PBS) and diluted to a concentration of 0.25 U/mL. After identification of the position using an image intensifier, three lumbar IVDs were randomly injected with a 29G needle, leaving three levels as negative controls. On average, 130  $\mu$ L (range 80-200  $\mu$ L) CABC-solution was delivered into each NP under manual pressure guidance. After suturing and recovery, animals were allowed to move freely in their cages and were fed *ad libitum*. Twelve weeks postoperatively the animals were sacrificed with an overdose of sodium pentobarbital, after which the lumbar spines were harvested en-bloc from T13 to L6. In order to confirm that mild degeneration had occurred, radiographic and MRI analysis was carried out.

### ***Radiological Analysis***

Before surgery and before autopsy, conventional lateral radiographs of the lumbar spine were obtained. To adjust for inter-animal differences and projection errors on the radiographs, a disc height index (DHI) was calculated as described earlier.<sup>22</sup> In short, disc and vertebral body height were derived by averaging 3 measurements of each IVD and vertebral body height. Subsequently, relative disc height was calculated as the ratio between average IVD height and

average caudal vertebral height. Finally, the relative disc heights on radiographs before autopsy were expressed as a percentage of the pre-operative disc heights. [DHI = preautopsy DHI / preoperative DHI \* 100%]. MRI scans were taken in sagittal direction, using a T2 weighted sequence and slice thickness of 3 mm on a 1.5 Tesla Siemens Symphony machine. MRI scans were analysed using the MRI index.<sup>24</sup> In short, the images were transferred to commercially available image processing software (OsiriX Imaging Software, [www.osirix-viewer.com](http://www.osirix-viewer.com)) where the NP was identified manually as region of interest. Surface area and signal intensity were then computed automatically and their product resulted in an MRI index for each IVD. In order to compare between MRI scans, values were expressed as ratios of a reference tube filled with demineralised water, which was scanned together with the goat spines (figure 1).

### ***Biomechanical Testing***

Biomechanical testing was performed using a mechanical testing device with a maximum capacity of 4 adjacent motion segments. To prepare specimens for testing, either T13 to L4 or L1 to L5 were isolated en-bloc after which the posterior and transverse processes were removed. Each spinal sample thus obtained, contained two CABC-injected and two healthy intervertebral discs and mechanical testing was carried out as described previously.<sup>25,26</sup> In short, the two outer vertebral bodies were embedded in a low melting point bismuth alloy and the lumbar spine was placed in a mechanical testing device (Instron 8872, Canton, MA, USA). Markers containing light-emitting diodes (LEDs) were positioned on each vertebral body and motions of the LEDs were recorded by an optoelectronic 3D movement registration system (Optotrak 3020, Northern Digital Inc, Waterloo ON). The lumbar spine was positioned in its neutral, horizontal position where the load was set to zero. Subsequently, moments of 1 Nm were gradually applied in flexion/extension, right and left lateral bending and right and left axial rotation with a rotation speed of 1°/s. During the experiments, the

spines were protected from drying out by spraying with 0.9% saline intermittently. Specimens were tested for 3 continuous cycles and the data from the third cycle were analysed using a customised program written in Matlab (Mathworks, Natick MA, USA). Movement in all three directions was plotted as a function of load in order to obtain load-deflection curves. The range of motion (ROM) of each segment was calculated from these curves as the motion in degrees between +1 and -1 Nm. The neutral zone stiffness (NZS) was calculated as the slope of the curve in the NZ after fitting a summed sigmoid function, as described previously.<sup>27</sup> When the neutral zone could not be defined, the stiffness was derived from the slope around 0 Nm (-0.5 to +0.5 Nm).

### ***Rheological Characterization***

The motion segments were stored at -20°C until the day of rheological testing. After thawing, IVDs were cut from the endplates with a surgical knife and NPs were isolated using a 9 mm circular trephine. Rheological testing was performed as described before<sup>21</sup> on a stress-controlled rheometer (Paar Physica MCR501; Anton Paar, Graz, Austria) in parallel plate configuration (20 mm diameter, 2–3 mm gap). To ensure good contact with both plates and prevent sample slipping, sandpaper was attached to the plates. Also, a compressive strain of 10% of initial NP height was applied, temporarily increasing the normal force to ~0.12 N. The tests were performed at 37°C in a humidified chamber. To exclude any time-dependent viscoelastic behaviour during the experiments, samples were first equilibrated for 5 minutes at a fixed frequency of 0.5 Hz applying 0.5% strain. Meanwhile, normal force returned to values below 0.03 N in all samples. Next, we performed frequency sweep measurements over an angular frequency range of 0.01–30 Hz at fixed strain amplitude of 0.5%. The shear modulus  $G^*$  follows from the ratio between shear stress ( $\sigma$ ) and strain amplitude ( $\gamma$ ).  $G^*$  is a complex quantity with an elastic storage modulus ( $G'$ ) and a viscous loss modulus ( $G''$ ). The ratio between  $G''$  and  $G'$ , indicating energy dissipation, is called the damping factor and equals the

tangent of the phase shift angle ( $\tan \delta$ ) between shear stress and strain (figure 2). As the sample diameters were smaller than the plates, the measured values had to be corrected before further evaluation using the same correction factor applied earlier.<sup>21</sup> Values for  $G^*$ ,  $G'$ ,  $G''$  and  $\tan \delta$  were taken from the frequency sweep at 1 Hz ( $2\pi$  rad/s). Finally, the stiffness of NP samples in (unconfined) compression was tested under static loading conditions. This was performed by applying compressive strain at a fixed velocity of 0.01 mm/s until a normal force of 50 N was reached. Data from compression testing were analysed as described previously.<sup>28</sup> Briefly, a compressive modulus at low strain was calculated by linear regression as the slope of the stress-strain curve from approximately 10 to 30% compressive strain. Compressive strain was calculated as  $1 - H/H_0$  ( $H$  = height and  $H_0$  = initial height) and stress was calculated as normal force divided by sample area.

### ***Water Content***

All samples were weighed after rheological testing as well as after freeze-drying (speedvac). Water content was defined as the difference between wet and dry weight, expressed as a percentage of wet weight.

### ***Statistical Analysis***

To analyse the differences between CABC-injected and control IVDs, independent Student's t-tests were used on the disc height and MRI indices. To compare outcome parameters from mechanical and viscoelastic experiments, a General Linear Model was used with goat number as random factor. The analyses were performed using SPSS Statistics version 17.0 (SPSS Inc., Chicago, IL, USA), where p-value below 0.05 was considered statistically significant.

### **Results**

All goats showed normal ambulatory activities on the first post-operative day. One goat developed a superficial wound infection four weeks after surgery. Treatment consisted of

subcutaneous antibiotics (Penicillin-Streptomycin) during five days and daily rinsing. The wound healed six weeks postoperatively and the animal did not show signs of illness, discomfort or pain during that period. Eventually, the superficial wound infection was considered not to be of influence as this goat did not appear as an outlier in any of the outcome parameters. Otherwise, goats appeared healthy and body weight was either maintained or increased during follow-up. At autopsy, no abnormalities were found, neither at the site of surgery, nor elsewhere. Macroscopically, no major indications of degenerative disc disease (e.g. osteophytes, endplate fractures) were identified.

### ***Radiology***

Disc height index of the CABC-injected IVDs decreased by 6% compared to control levels (figure 3). This difference was statistically significant ( $p < 0.01$ ). No endplate fractures or osteophytes were observed in any of the lumbar spines on radiological analysis. The MRI index of CABC-injected IVDs was significantly lower than controls, with an average difference of 22% ( $p < 0.001$ ; figure 3). On MR imaging, no gross aberrations were observed on the lumbar spine. All cartilaginous endplates were intact and no annular tears were seen.

### ***Biomechanical testing***

Load-deflection curves were plotted for each tested IVD ( $n=32$ ) in all three directions: flexion/extension (FE), lateral bending (LB) and axial rotation (AR). In 9 of the resulting 96 curves the neutral zone had to be indicated manually because the maxima in the second derivative were not adequately identified. In 9 other plots, no maxima in the second derivative (due to lack of a double sigmoid function) were identified at all and the NZ stiffness was calculated as the slope of the curve around 0 Nm. In two curves fitting was not possible at all, hence the curve resulting from the downward movement of cycle 3 was used to calculate NZS. In lateral bending and axial rotation, the NZS decreased significantly with mild degeneration by 31% and 27% respectively. ROM increased by 23% ( $p < 0.001$ ) for lateral

bending and by 32% ( $p < 0.01$ ) in axial rotation. No statistically significant differences were observed in flexion/extension after CABC-injection (figure 4).

### ***Rheometry***

In all samples, the elastic storage modulus  $G'$  was three to four times larger than the viscous loss modulus  $G''$  indicating a more solid than liquid behaviour of the NP. This is also reflected by the damping factor  $\tan \delta$  that remained at  $0.30 \pm 0.02$  with no significant difference between the CABC-injected and control NPs. The variation in the complex shear modulus  $G^*$  between goats was remarkably large (figure 5). In spite of this, a statistically significant ( $p < 0.05$ ) decrease of circa 10% in both elastic and viscous moduli was observed in mildly degenerated NPs after applying a General Linear Model analysis with “goat” as random factor (figure 6). One goat stood out of this tendency and showed a non-significant increase in the rheological parameters. To quantify the response to compressive loads, we calculated the compressive modulus as the slope of the stress-strain curve at low strain. The mean compressive modulus was  $0.46 \pm 0.17$  kPa. No significant difference was observed in this parameter between CABC-injected and control NPs.

### ***Water content***

The relative water content of the NPs, calculated as loss of weight after freeze-drying was not different between CABC-injected ( $74.9 \pm 1.4\%$ ) and healthy samples ( $74.7 \pm 1.1\%$ ).

Furthermore, water content was not correlated to any of the rheological parameters.

### **Discussion**

We evaluated the biomechanical characteristics of spinal motion segments and viscoelastic properties of the nucleus pulposus in healthy and mildly degenerated goat IVDs. Imaging techniques were applied to assess a decrease in disc height and a lower signal intensity of the NP on MRI. These two findings confirmed the presence of mild degeneration

after CABC injection into the IVDs of the large animal model as described before.<sup>22,23</sup>

Moreover, we observed a decrease in neutral zone stiffness and an increase in the range of motion after inducing mild disc degeneration. This further corroborates our disc degeneration model, as mild degeneration is generally correlated with increased mobility of the IVD in previous biomechanical research on both animal<sup>29,30</sup> and human spines<sup>31-35</sup>.

Rheological tests were performed on isolated nuclei pulposi, resulting in elastic (storage) and viscous (loss) moduli in the same range as both human and goat values from previous studies.<sup>21,36</sup> However, we found a remarkably large inter-animal variation in viscoelastic moduli. As the measured values are far more consistent within each goat, this suggests that the large differences are due to varying animal characteristics, rather than an artefact of sensitive measurement methods. Moreover, in a comparable study on cadaveric human NP material, an even larger range of values for the moduli was observed.<sup>36</sup> Whether inter-individual environmental differences, congenital properties or specific circumstances during (embryological) development can account for this wide variation between subjects remains to be elucidated.

In spite of the relatively large inter-animal differences, we observed a modest but significant decrease in viscoelastic moduli (~10%) after mild degeneration. Interestingly, this is in contrast to an earlier study on human cadaveric material,<sup>37</sup> where shear moduli increased with age and degeneration. In our model, goat discs are mildly degenerated (Thompson grade II-III)<sup>23</sup> whereas Iatridis et al. reported degeneration up to Thompson grade V. In addition, degeneration in human IVDs develops over many years, whilst induction of the mild degeneration in this study was achieved within 12 weeks. This is a relatively short period for extracellular matrix changes – like collagen type I deposition – to develop, resulting in viscoelastic changes. Possibly, spinal motion segments lose stiffness at an early degenerative stage, due to a slight decrease in NP viscoelastic moduli, while after a longer period

degeneration is characterised by an increase in elastic modulus. In our study, the damping factor  $\text{Tan } \delta$  (ratio between the viscous and elastic moduli), indicative of energy dissipation, remained unchanged with mild degeneration. Again, this differs from human cadaveric studies,<sup>37</sup> where a decrease in energy dissipation with increasing degeneration was observed. In other words, the viscoelastic behaviour of degenerated human NPs shifted from “fluid-like” to more “solid-like”, whereas our goat NPs did not show this transition. This contrast might be explained by the difference in duration of the degenerative processes as well. Eventually, this shift could also arise in the goat model by the formation of fibrous tissue. After all, our model has previously demonstrated increased gene expression of collagen type I in severely degenerated discs.<sup>38</sup> The unaltered energy dissipation is also in accordance with the unchanged water content between healthy and degenerated NPs, measured as the relative decrease in weight before and after freeze-drying.

Recently, other researchers also found unaltered water content in chemically degenerated rat IVDs<sup>39</sup> confirmed in goat IVDs by unpublished data from our group. Both quantified the water content of the NP, determined by weighing before and after dehydration. Chemically induced degeneration is characterised by a loss of glycosaminoglycans (GAG) from the NP due to cleavage by CABC, injected into the IVDs. Previous studies have documented this proteoglycan loss as a decreased GAG-collagen ratio (30:1 to 15:1)<sup>38</sup> and as a reduced GAG content in the NP (43% decrease)<sup>30</sup>. As the declining GAG content is followed by diffusion of water out of the NP, water loss will be proportional to the lost proteoglycan amount. As a consequence, (relative) water content remains unchanged. In more advanced stages of degeneration the increase of collagen type I in the NP might increase the protein content, explaining the observation of loss of water content and increased elastic modulus by others.<sup>37</sup>

Injection of a 0.25 U/ml CABC solution into goat IVDs results in a relatively mild degeneration compared to the severity of the degenerative process in other (human) studies. Our model was deliberately designed to mimic a very mild degeneration, as we consider this mild process to be reversible and with that, suitable for potential regenerative treatment. The drawback of inducing a more severe degeneration is the potential extra damage to endplate or annulus fibrosus (AF) that might occur, rendering regenerative strategies less opportune. Nevertheless, this mild grade of degeneration is sufficient to produce significantly altered imaging, histological, biochemical and mechanical outcome parameters. Hence, our animal model represents a valid method for investigating mild IVD degeneration and subsequent testing of evolving regenerative therapies for NP repair.

Unlike the relatively small decrease in viscoelasticity, segmental biomechanical characteristics changed consistently (circa 30% decrease in NZ stiffness and increase in ROM) with mild degeneration. Consequently, the impact of viscoelastic properties on the biomechanical behaviour of the whole spinal motion segment is marginal. We suggest that hydrostatic pressure in the NP influences biomechanical behaviour of the segments more than viscoelasticity of the NP. Loss of hydrostatic pressure has been identified before as a cause of biomechanical changes.<sup>40</sup> In the introduction, we already illustrated the importance of biochemical and mechanical stimuli for the direction of regenerative cells in IVD matrix tissue. Therefore, when developing regenerative therapies, emphasis might be shifted towards the mechanobiological interaction of scaffolds with regenerative cells, instead of mimicking native nucleus pulposus material properties.

In conclusion, we established mild degeneration in lumbar intervertebral discs in a goat model as confirmed by radiology and biomechanical testing. We observed a slight decrease in both elastic and viscous moduli, but the ratio between these remained unchanged, indicating that the NPs did not become more fluid-like nor elastic-like. This is consistent with our

measurements on the water content of the nuclei pulposi, which also remained unchanged. The large variability between animals in viscoelasticity, but not in segmental biomechanical characteristics, implies that the influence of viscoelasticity within the NP on the mechanical behaviour of the whole spinal motion segment is marginal. Therefore, when developing NP replacement materials, the focus should be on other design criteria for NP regeneration, like biochemical cues and swelling pressure.

### **Acknowledgments**

The authors thank Klaas-Walter Meijer and Paul Sinnige for assistance with the surgeries, Baldomero Alonso Latorre for help with rheology, and Susanne van Engelen for her help with biomechanical analysis. This study was funded by the European Commission as part of the 7th framework programme (FP7; #246351; NPmimetic). None of the authors has a conflict of interest to declare.

### **References**

1. Chan WCW, Sze KL, Samartzis D, et al. 2011. Structure and biology of the intervertebral disk in health and disease. *Orthop Clin North Am* 42: 447-464, vii.
2. Cheung KMC, Karppinen J, Chan D, et al. 2009. Prevalence and pattern of lumbar magnetic resonance imaging changes in a population study of one thousand forty-three individuals. *Spine* 34: 934-940.
3. Takatalo J, Karppinen J, Niinimäki J, et al. 2011. Does lumbar disc degeneration on magnetic resonance imaging associate with low back symptom severity in young finnish adults? *Spine* 36: 2180-2189.
4. Roughley PJ. 2004. Biology of intervertebral disc aging and degeneration: involvement of the extracellular matrix. *Spine* 29: 2691-2699.

5. Bron JL, Vonk LA, Smit TH, Koenderink GH. 2011. Engineering alginate for intervertebral disc repair. *J Mech Behav Biomed Mater* 4: 1196-1205.
6. Calderon L, Collin E, Velasco-Bayon D, et al. 2010. Type II collagen-hyaluronan hydrogel--a step towards a scaffold for intervertebral disc tissue engineering. *Eur Cell Mater* 20: 134-148.
7. Huang B, Zhuang Y, Li C-Q, et al. 2011. Regeneration of the Intervertebral Disc with Nucleus Pulposus Cell-seeded Collagen $\alpha$ /Hyaluronan/Chondroitin-6-sulfate tri-copolymer Constructs in a Rabbit Disc Degeneration Model. *Spine*.
8. Moss IL, Gordon L, Woodhouse KA, et al. 2011. A novel thiol-modified hyaluronan and elastin-like polypeptide composite material for tissue engineering of the nucleus pulposus of the intervertebral disc. *Spine* 36: 1022-1029.
9. Park S-H, Cho H, Gil ES, et al. 2011. Silk-Fibrin/Hyaluronic Acid Composite Gels for Nucleus Pulposus Tissue Regeneration. *Tissue Engineering Part A*.
10. Anderson DG, Risbud MV, Shapiro IM, et al. 2005. Cell-based therapy for disc repair. *Spine J* 5: 297S-303S.
11. Hohaus C, Ganey TM, Minkus Y, Meisel HJ. 2008. Cell transplantation in lumbar spine disc degeneration disease. *Eur Spine J* 17 Suppl 4: 492-503.
12. Masuda K, Lotz JC. 2010. New challenges for intervertebral disc treatment using regenerative medicine. *Tissue Eng Part B Rev* 16: 147-158.
13. Urban JPG, Smith S, Fairbank JCT. 2004. Nutrition of the intervertebral disc. *Spine* 29: 2700-2709.
14. Setton LA, Chen J. 2004. Cell mechanics and mechanobiology in the intervertebral disc. *Spine* 29: 2710-2723.
15. McBeath R, Pirone DM, Nelson CM, et al. 2004. Cell shape, cytoskeletal tension, and RhoA regulate stem cell lineage commitment. *Dev Cell* 6: 483-495.
16. Engler AJ, Sen S, Sweeney HL, Discher DE. 2006. Matrix elasticity directs stem cell lineage specification. *Cell* 126: 677-689.
17. Gao L, McBeath R, Chen CS. 2010. Stem cell shape regulates a chondrogenic versus myogenic fate through Rac1 and N-cadherin. *Stem Cells* 28: 564-572.

18. Ghosh K, Pan Z, Guan E, et al. 2007. Cell adaptation to a physiologically relevant ECM mimic with different viscoelastic properties. *Biomaterials* 28: 671-679.
19. Gilchrist CL, Darling EM, Chen J, Setton LA. 2011. Extracellular matrix ligand and stiffness modulate immature nucleus pulposus cell-cell interactions. *PLoS ONE* 6: e27170.
20. Iatridis JC, Setton LA, Weidenbaum M, Mow VC. 1997. The viscoelastic behavior of the non-degenerate human lumbar nucleus pulposus in shear. *J Biomech* 30: 1005-1013.
21. Bron JL, Koenderink GH, Everts VE, Smit TH. 2009. Rheological characterization of the nucleus pulposus and dense collagen scaffolds intended for functional replacement. *J Orthop Res* 27: 620-626.
22. Hoogendoorn RJW, Wuisman PIJM, Smit TH, et al. 2007. Experimental intervertebral disc degeneration induced by chondroitinase ABC in the goat. *Spine* 32: 1816-1825.
23. Hoogendoorn RJW, Helder MN, Kroeze RJ, et al. 2008. Reproducible long-term disc degeneration in a large animal model. *Spine* 33: 949-954.
24. Sobajima S, Kempel JF, Kim JS, et al. 2005. A slowly progressive and reproducible animal model of intervertebral disc degeneration characterized by MRI, X-ray, and histology. *Spine* 30: 15-24.
25. Krijnen MR, Mensch D, van Dieen JH, et al. 2006. Primary spinal segment stability with a stand-alone cage: in vitro evaluation of a successful goat model. *Acta Orthop* 77: 454-461.
26. Smolders LA, Bergknut N, Kingma I, et al. 2011. Biomechanical evaluation of a novel nucleus pulposus prosthesis in canine cadaveric spines. *Veterinary journal (London, England : 1997)*.
27. Smit TH, van Tunen MS, van der Veen AJ, et al. 2011. Quantifying intervertebral disc mechanics: a new definition of the neutral zone. *BMC Musculoskelet Disord* 12: 38.
28. Kreger ST, Voytik-Harbin SL. 2009. Hyaluronan concentration within a 3D collagen matrix modulates matrix viscoelasticity, but not fibroblast response. *Matrix Biol* 28: 336-346.
29. Lü DS, Shono Y, Oda I, et al. 1997. Effects of chondroitinase ABC and chymopapain on spinal motion segment biomechanics. An in vivo biomechanical, radiologic, and histologic canine study. *Spine* 22: 1828-1834; discussion 1834-1825.
30. Boxberger JJ, Auerbach JD, Sen S, Elliott DM. 2008. An in vivo model of reduced nucleus pulposus glycosaminoglycan content in the rat lumbar intervertebral disc. *Spine* 33: 146-154.

31. Friberg S, Hirsch C. 1992. Anatomical and clinical studies on lumbar disc degeneration. 1950. Clin Orthop Relat Res: 3-7.
32. Ferguson SJ, Steffen T. 2003. Biomechanics of the aging spine. Eur Spine J 12 Suppl 2: S97-S103.
33. Tsantrizos A, Ito K, Aebi M, Steffen T. 2005. Internal strains in healthy and degenerated lumbar intervertebral discs. Spine 30: 2129-2137.
34. Quint U, Wilke H-J. 2008. Grading of degenerative disk disease and functional impairment: imaging versus patho-anatomical findings. Eur Spine J 17: 1705-1713.
35. Brown MD, Holmes DC, Heiner AD. 2002. Measurement of cadaver lumbar spine motion segment stiffness. Spine 27: 918-922.
36. Iatridis JC, Weidenbaum M, Setton LA, Mow VC. 1996. Is the nucleus pulposus a solid or a fluid? Mechanical behaviors of the nucleus pulposus of the human intervertebral disc. Spine 21: 1174-1184.
37. Iatridis JC, Setton LA, Weidenbaum M, Mow VC. 1997. Alterations in the mechanical behavior of the human lumbar nucleus pulposus with degeneration and aging. J Orthop Res 15: 318-322.
38. Hoogendoorn RJW, Zandieh Doulabi BZ, Huang CL, et al. 2008. Molecular changes in the degenerated goat intervertebral disc. Spine 33: 1714-1721.
39. Boxberger JI, Sen S, Yerramalli CS, Elliott DM. 2006. Nucleus pulposus glycosaminoglycan content is correlated with axial mechanics in rat lumbar motion segments. J Orthop Res 24: 1906-1915.
40. Adams MA, Roughley PJ. 2006. What is intervertebral disc degeneration, and what causes it? Spine 31: 2151-2161.

## **Figures & legends**

Figure 1. Images from a representative part of an MRI scan showing two control IVDs (left) and two injected IVDs (right). On the second image, MRI index lines are drawn.

Figure 2. Schematic showing the associations between various rheological parameters: complex shear modulus ( $G^*$ ), elastic ( $G'$ ) and viscous modulus ( $G''$ ), phase shift angle ( $\delta$ ), shear stress ( $\sigma$ ) and strain amplitude ( $\gamma$ ).

Figure 3. Disc height and MRI index of control IVDs (n=24) and levels injected with CABC (n=24), data plotted as mean and SD. [\*\* p<0.01; \*\*\* p<0.001]

Figure 4. Neutral zone stiffness and range of motion in flexion/extension, lateral bending and axial rotation for CABC-injected and control intervertebral discs. Data plotted as mean and SD. [\* p<0.05; \*\* p<0.01; \*\*\* p<0.001]

Figure 5. Inter-animal variation in the shear modulus ( $G^*$ ) and difference between control and CABC nucleus pulposus. Each box represents two IVDs (n=2, in total n=32).

Figure 6. Elastic storage ( $G'$ ) and viscous loss modulus ( $G''$ ) of CABC-injected NPs compared to healthy control levels. A slight decrease ( $p < 0.05$ ) in both the elastic and viscous modulus was observed after analysis with a General Linear Model. (n=2 per group, in total n=32).

# Figures

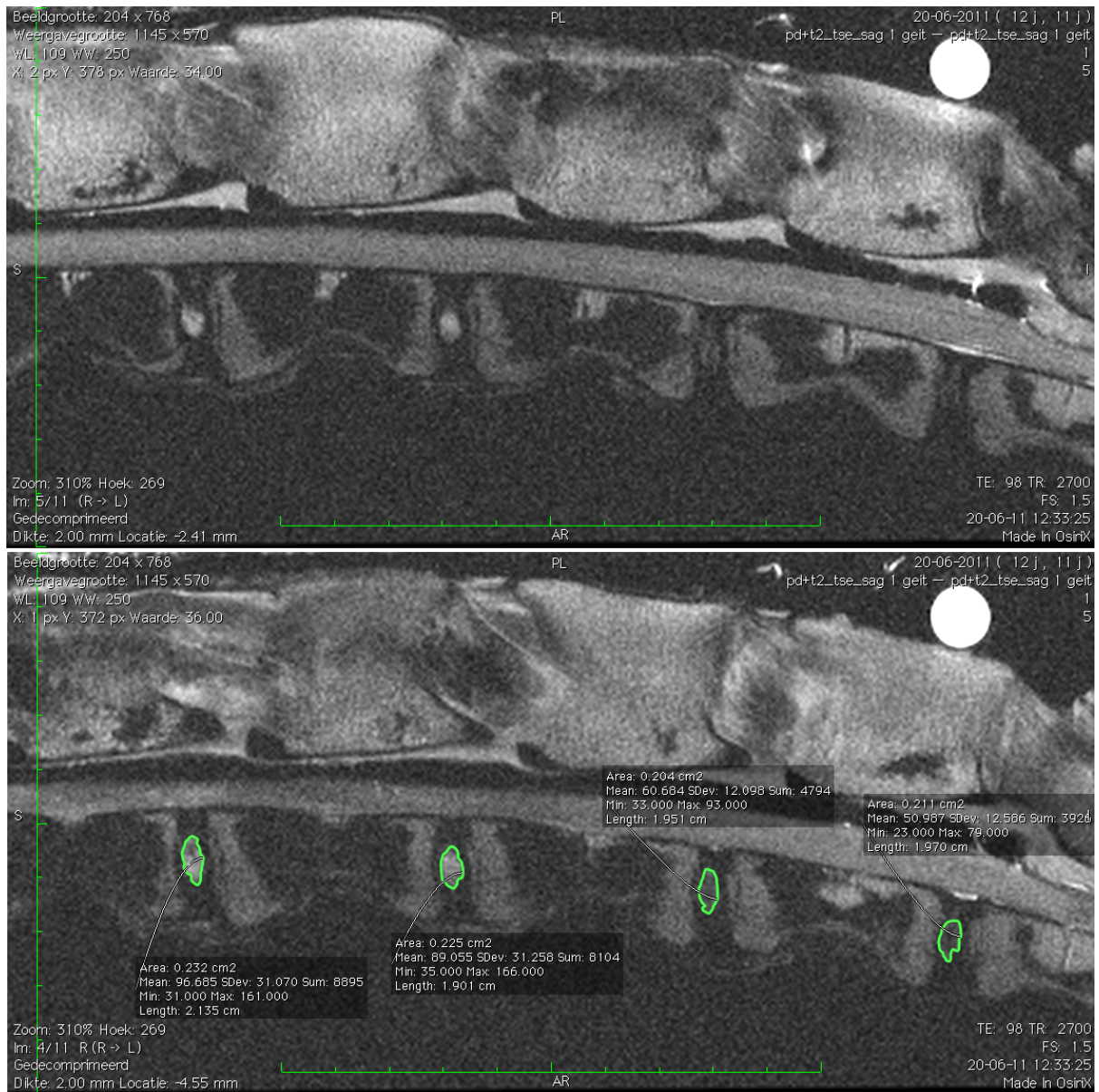


Figure 1.

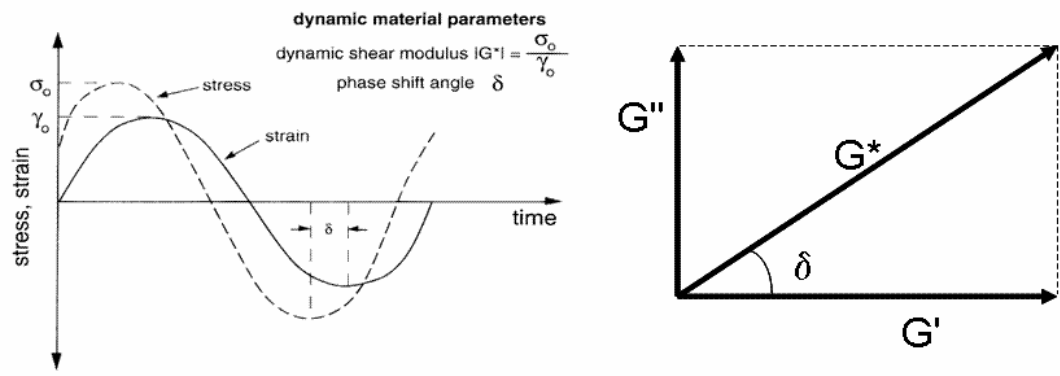


Figure 2.

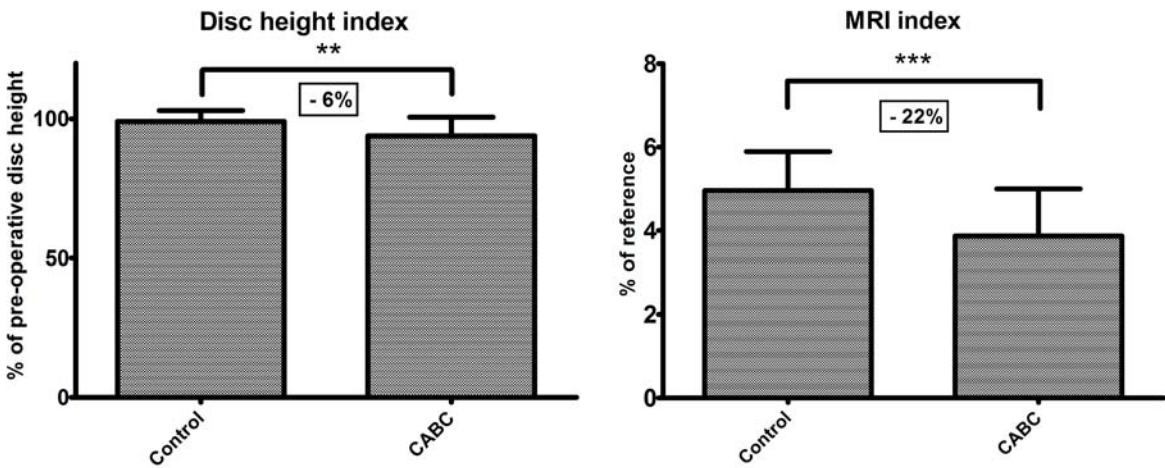


Figure 3.

## Neutral zone stiffness (NZS) & range of motion (ROM)

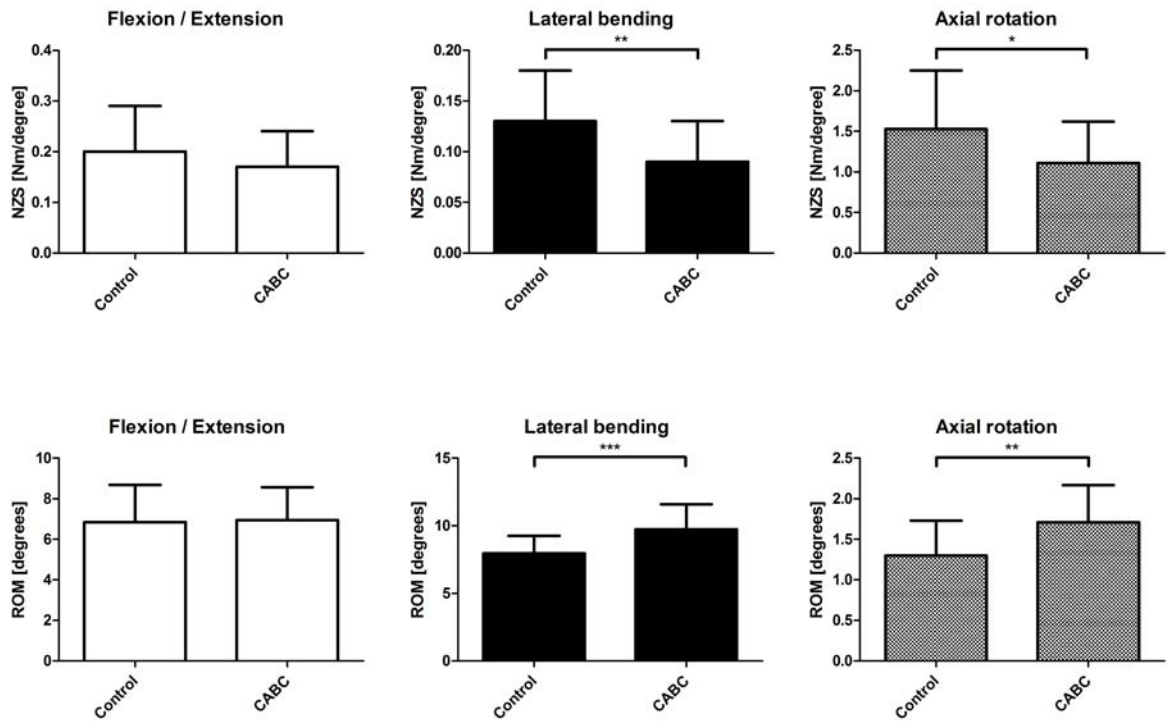


Figure 4.

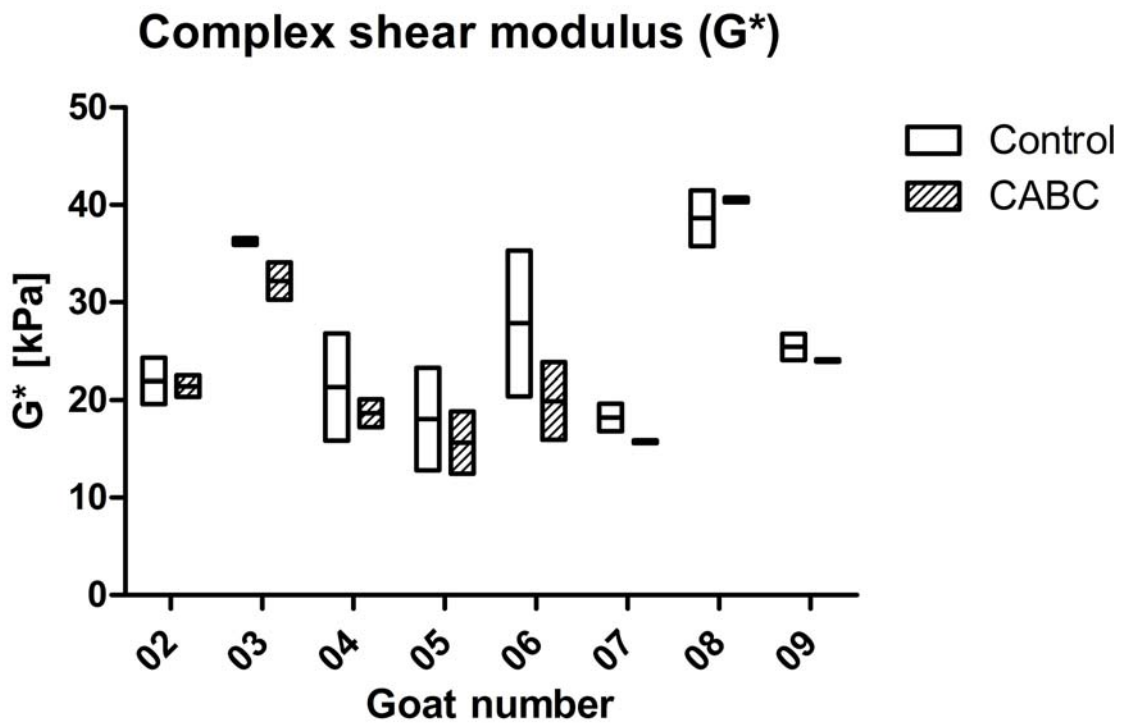


Figure 5.

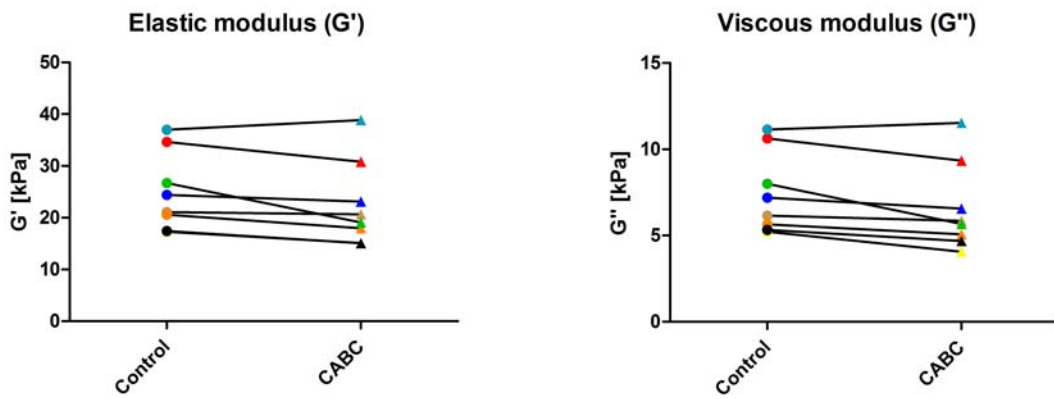


Figure 6.